Optical and scintillation properties of large $LuAlO_3:Ce^{3+}$ crystals

1998 J. Phys.: Condens. Matter 10 3061

(http://iopscience.iop.org/0953-8984/10/13/022)

J. Phys.: Condens. Matter **10** (1998) 3061–3073. Printed in the UK PII: S0953-8984(98)88720-1

Optical and scintillation properties of large $LuAlO_3:Ce^{3+}$ crystals

C Dujardin†, C Pedrini†, W Blanc†, J C Gâcon†, J C van't Spijker‡, O W V Frijns‡, C W E van Eijk‡, P Dorenbos‡, R Chen§, A Fremout§, F Tallouf§, S Tavernier§, P Bruyndonckx§ and A G Petrosyan‖

† Laboratoire de Physico-Chimie des Matériaux Luminescents, UMR No 5620, CNRS et Université Claude Bernard Lyon I, 69622 Villeurbanne, France

‡ Delft University of Technology, Mekelweg 15, 2629JB Delft, The Netherlands

§ Inter-University Institute of High Energy, VUB, Pleinlaan 2, B-1050, Brussels, Belgium

‖ Institute for Physical Research, Armenian National Academy of Science, 378410 Ashtarak-2, Armenia

Received 27 October 1997, in final form 5 January 1998

Abstract. The $LuAlO_3:Ce^{3+}$ system has been shown to be a promising scintillator for medical imaging devices. Recently, efforts were focused on the improvement of its scintillating properties. Several large crystals with various cerium concentrations were grown. Absorption and excitation spectra were measured in a range extending from the visible to the vacuum ultraviolet (VUV). Emission spectra, fluorescence decay times and light yields, both under γ-ray and x-ray excitation, were measured under various experimental conditions. A reabsorption process is shown to take place in this material. This process is responsible for the observed decrease of the light yield when increasing the size of the sample.

Introduction

Many recent investigations have been devoted to the $LuAlO_3:Ce^{3+}$ system, which is a promising new scintillator [1–13]. This material has a density of 8.34 g cm^{-3}, a photoelectric fraction of 32.1% at 511 keV and a UV fluorescence decay time of 18 ns. This performance makes this crystal a very good candidate for positron emission tomograph (PET) cameras used in medical imaging [3]. However, the production of this material has not been optimized yet. More effort is needed to grow high-optical-quality samples of large size. This will involve the optimization of the doping level, and the control of the cerium valence state and of the unintentionally added impurities.

Several single crystals with various sizes and cerium concentrations were grown in the framework of the Crystal Clear Collaboration supported by CERN. The present paper reports the results of spectroscopic investigations and light yield measurements on this new series of samples.

1. Crystal growth

Cerium-doped lutetium orthoaluminate crystals were grown using the vertical Bridgman technique as previously reported [10]. Due to the low Ce^{3+} distribution coefficient ($k = 0.17 \pm 0.05$), the growth of single crystals with a sufficiently high doping level

0953-8984/98/133061+13$19.50

is difficult. Our ultimate goal was to find crystallization conditions which would ensure the required Ce^{3+} concentration in the crystal while maintaining its optical quality and mechanical ruggedness. The influence of the experimental growth parameters (growth rate, melt composition, thermal gradients and gaseous atmosphere) on the optical quality of the crystal, and on the concentration and distribution of the Ce^{3+} ions in the crystal, was studied. As a result, 60 mm long rods of high optical quality could be grown. They are colourless single-phase crystals, free of twins and light scattering.

The Ce concentration in the crystals was measured using the spectral emission technique employing standard samples with a cerium concentration between 0.05 and 1 at.%. As is well known, this technique gives an overall cerium concentration independent of the valence state. The Ce distribution, measured in crystal grown from a melt with 0.5 at.% of initial Ce concentration, is well described by the usual freezing equation. Four large samples (1 to 4) were given parallelepipedic shapes and polished. End to end variation of the Ce concentration was observed to be within 0.01 at.% for sample 1 and 0.03 at.% for sample 2. In addition, six thin platelets were cut (samples 5 to 10). Samples 1 and 6, on one hand, and 2 and 7, on the other hand, were cut from two different parts of the same boule. Samples 3 and 9 were cut from another boule and samples 4 and 10 were obtained from a third boule. Samples 5 and 8 were cut from two other boules. The dimensions and Ce doping levels of the different samples under investigation are given in table 1. Spectroscopic investigations on a thin undoped sample (0) were also conducted for the purpose of comparison.

Table 1. Ce doping levels and dimensions of the samples under investigation.

	0	1	2	3	4	5	6	7	8	9	10
Ce concentration (at.%)	0	0.13	0.19	0.47	0.9	0.005	0.13	0.2	0.28	0.47	0.9
Length or thickness (mm)[a]	0.705	10	10	10	16	0.365	0.130	0.120	0.105	0.600	0.540

[a] Samples 1 to 4 are parallelepipedic and measure 5×5 mm^2 times the length given in this table.

2. Vacuum ultraviolet and visible spectroscopy

Absorption spectra from the near infrared up to the ultraviolet (UV) domain were measured using a CARY model 2300 spectrophotometer. Emission spectra under laser excitation were obtained using a dye laser pumped by a frequency-doubled Q-switch Nd:YAG pulsed laser from Quantel. The fluorescent emission was analysed through a 1 m Hilger and Watts monochromator monitored by a computer. Optical excitation in the UV was achieved either by doubling the frequency of the visible beam at the output of the dye laser or, if necessary, by mixing the frequency of this beam with that of the infrared Nd:YAG laser beam. Excitation spectra in the VUV were obtained using the synchrotron radiation facilities at the Laboratoire pour l'Utilisation du Rayonnement Electromagnétique (LURE) at Orsay (France), as described elsewhere [14].

The room-temperature absorption spectra of $LuAlO_3$:Ce^{3+} with various cerium concentration levels are presented in figure 1(A). These spectra exhibit five bands in the 200–350 nm region, which are unambiguously assigned to Ce^{3+} $4f \rightarrow 5d$ bands. The dependence of the absorption coefficient on the excitation energy was deconvoluted assuming that the five $4f \rightarrow 5d$ bands have a Gaussian shape. The result of this deconvolution (figure 1(B)) shows clearly evidence for an absorption tail on the low-energy side, which does not originate from Ce^{3+} $4f \rightarrow 5d$ transitions. Subtracting the contribution of this smooth

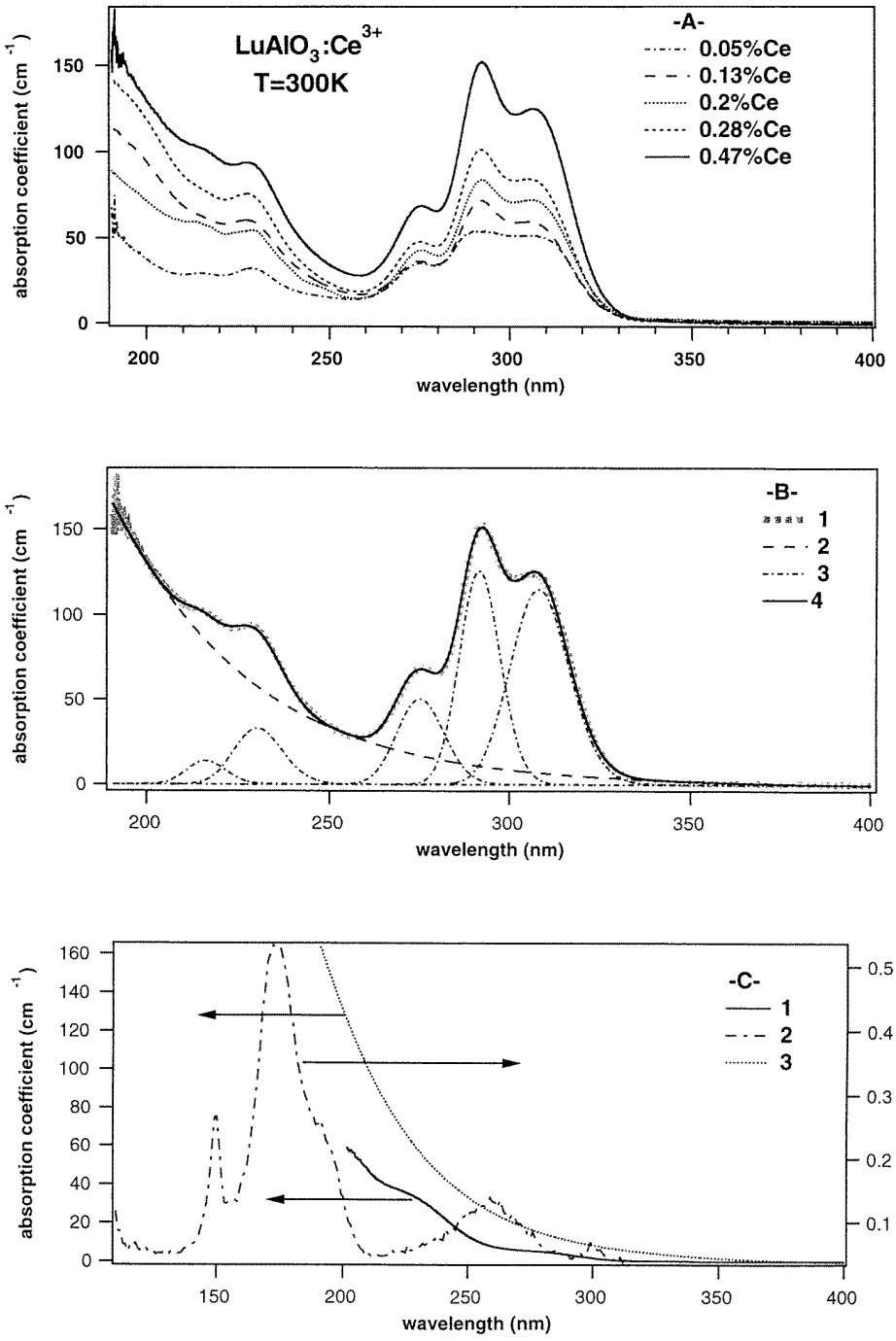

Figure 1. (A) $LuAlO_3:Ce^{3+}$ room-temperature absorption spectra for Ce concentrations ranging from 0.05 to 0.47 at.%. (B) Deconvolution of the absorption spectrum of sample 3: experimental (1), residual absorption tail (2), 4f $\rightarrow$ 5d Gaussian components (3), resulting fit (4). (C) $LuAlO_3$ undoped sample. Room-temperature absorption spectrum (1) and excitation spectrum of the red emission at 650 nm (2). The residual absorption obtained from the fit in figure 1(B) is also shown (3).

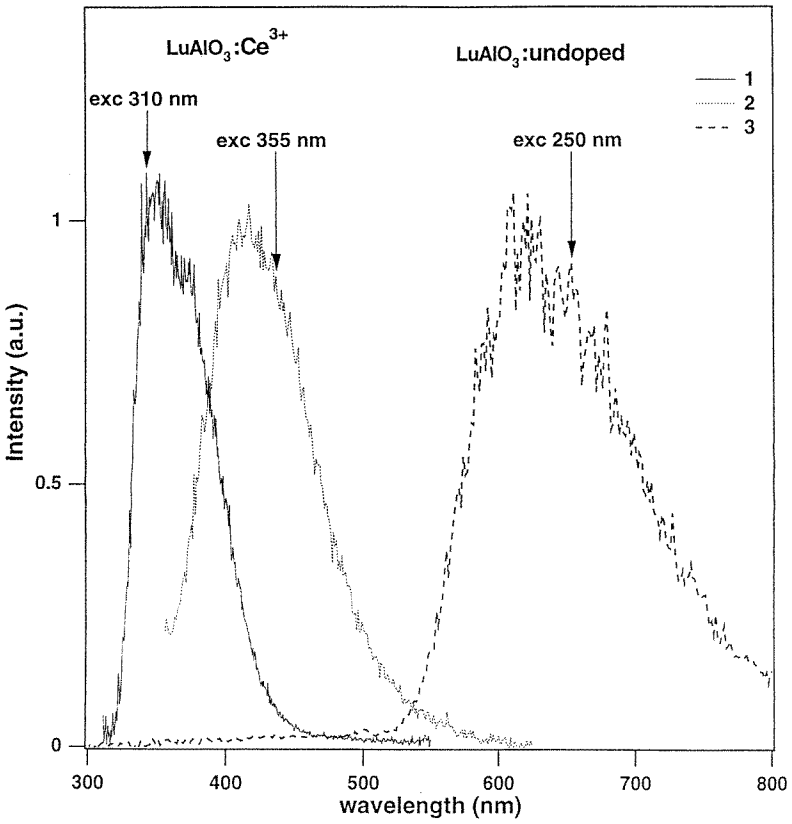

Figure 2. Room-temperature emission spectra of pure and Ce^{3+}-doped $LuAlO_3$ samples. $LuAlO_3$:Ce^{3+}: laser excitation at 310 nm (1) and 355 nm (2). Undoped sample: laser excitation at 250 nm (3).

tail from the experimental absorption spectrum reproduces the excitation spectrum of the Ce^{3+} fluorescence in the spectral interval under consideration. The presence of such an absorption tail has already been observed in both cerium-doped $YAlO_3$ and $LuAlO_3$ crystals [4, 15]. The origin of this additional broad band was tentatively assigned to Ce^{4+} ions by Gumanskaya *et al* [15]. In the case of our samples, the Ce^{3+} 5d $\rightarrow$ 4f fluorescence is rather poorly excited with a laser beam centred at 250 nm, though the measured absorption coefficient at this wavelength is not zero. This absorption coefficient increases from 15 to 30 cm^{-1}, when raising the cerium concentration, but this concentration dependence is not linear, in contradiction to what is observed for the absorption coefficient at the peak of the lowest 4f $\rightarrow$ 5d band (310 nm). The absorption tail under consideration should not therefore originate from Ce^{4+} ions only but also from other centres, the nature of which is to be determined. This conclusion is also supported by the observation that the absorption coefficient at 310 nm obtained at zero Ce concentration by extrapolating the data shown in figure 1(A) is not zero.

It follows from the above that a laser beam centred at 250 nm should excite predominantly those centres responsible for this absorption tail which extends up to 400 nm. Beside a weak Ce^{3+} UV fluorescence, this excitation induces a broad emission band peaking around 600 nm. Such a red emission was also observed for the undoped $LuAlO_3$ material

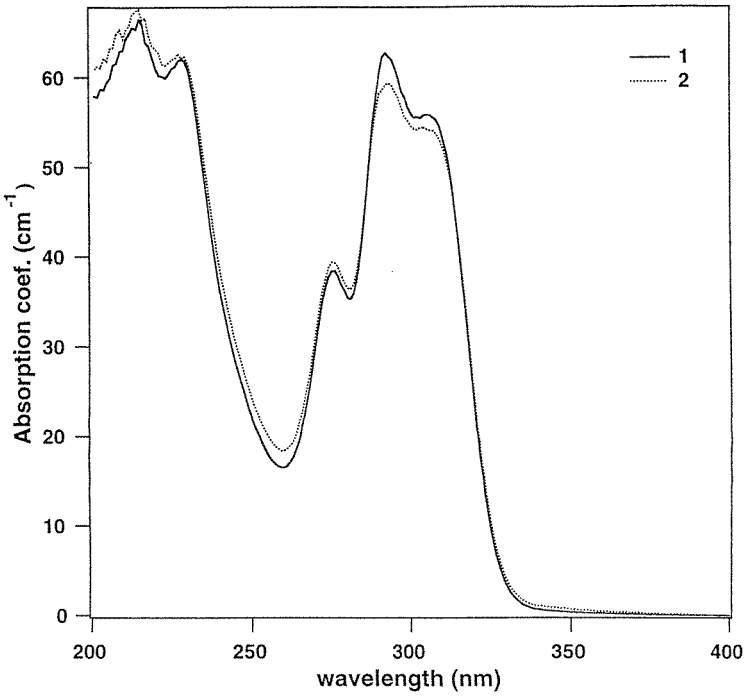

Figure 3. $LuAlo_3:Ce^{3+}$ room-temperature absorption spectrum before (1) and after (2) thermal treatment in air.

(figure 2), and for $LuAlO_3$ samples doped either with Nd^{3+} or Pr^{3+} ions. In all these samples, this emission has a purely exponential decay with a time constant around 13 μs. These slow fluorescence decays were measured using pulsed laser excitation at 250 nm (pulse frequency and duration 10 Hz and 10 ns, respectively), and a model SR430 multichannel scaler from Stanford Research Systems. Baryshevsky *et al* reported the observation of such a broad red emission band peaking at 600 nm in a cerium-doped $YAlO_3$ crystal under x-ray excitation [16]. The shape of the band which they observed was very similar to that appearing in the emission spectrum of the undoped $LuAlO_3$ sample under 250 nm excitation shown in figure 2. These authors attributed this emission to colour centres which were shown to strongly depend on the method used for growing the crystals.

The excitation spectrum of the red emission in the undoped sample was achieved using the synchrotron radiation at LURE. In the region between 100 and 400 nm, it exhibits five main bands peaking at 300, 260, 191, 175 and 150 nm, respectively (figure 1(C)). Moreover, the strongest band peaking at 175 nm shows a hump at 189 nm. The narrow band around 150 nm might originate from the creation of excitons which then transfer their energy to the centres responsible for the red emission under consideration. The absorption spectrum of the undoped $LuAlO_3$ sample is also shown in figure 1(C).

We also performed a thermal treatment in air at 1000 °C for 5 hours on a sample cut from the same boule as samples 4 and 10. Such a treatment should favour the conversion of trivalent cerium to the tetravalent state without changing the perovskite phase to the garnet phase. The absorption spectrum of this sample was measured before and after treatment. As a matter of fact, the thermal treatment results in increasing the absorption around 250 nm, as well as decreasing it around 300 nm, but the induced variations are not significant enough to

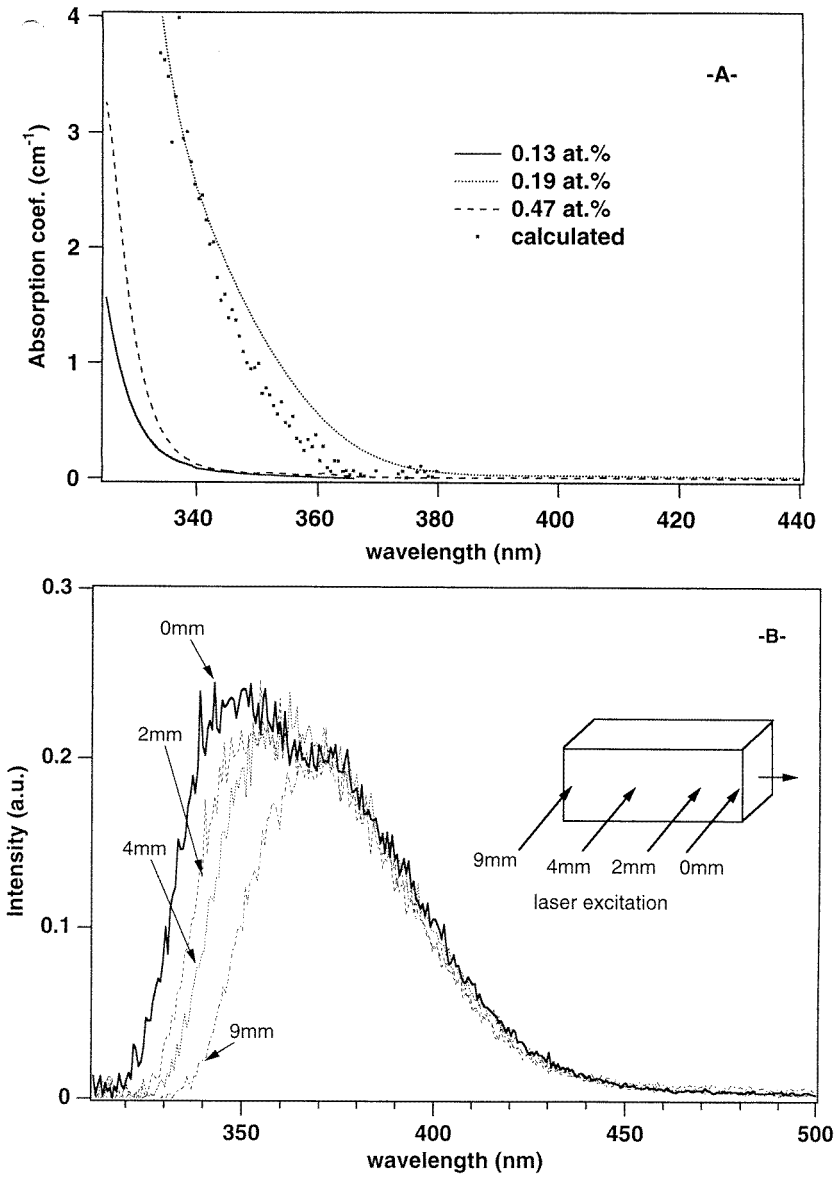

Figure 4. (A) Absorption tail of large samples (1–3) measured at room temperature. (B) Dependence on the position of the laser impact point of the room-temperature emission spectrum of sample 2 under laser excitation at 310 nm.

prove that part of the absorption tail might be due to Ce^{4+} ions (see figure 3). Moreover, the presence of cerium in the tetravalent state would not explain why the additional absorption band also appears in the spectra of undoped as well as Pr^{3+} and Nd^{3+}-doped samples and why the red fluorescence associated with the absorption at 250 nm is also observed in these cerium-free samples.

The x-ray-induced emission spectra of $LuAlO_3:Ce^{3+}$ crystals were observed to be dependent on the thickness of the samples [6]. The spectral overlap between the Ce^{3+}

emission and the absorption tail extending up to 400 nm was shown to be responsible for the major part of this dependence. The measured absorption coefficient between 325 and 400 nm does not appear to be proportional to the cerium concentration, as shown in figure 4(A) for three of our large samples. Choosing sample 2 (0.19 at.%), which exhibits the higher absorption in this spectral interval, we analysed the influence on the emission spectrum under laser excitation at 310 nm of the distance between the point of impact of the impinging laser beam and the face through which the fluorescence is coming out of the crystal. Thanks to the large size of the sample, this distance could be made as large as 10 mm. The results of these experiments are reported in figure 4(B). The peak corresponding to Ce^{3+} transitions between the lowest 5d level and the $^2F_{7/2}$ multiplet is progressively rubbed out when increasing the distance under consideration. On the other hand, the long-wavelength part of the spectrum involving mostly the $^2F_{5/2}$ ground level remains unchanged. This observation clearly demonstrates that Ce^{3+} radiative $5d \rightarrow 4f$ transitions are reabsorbed in the sample under investigation. From the 0 and 9 mm emission spectra shown in figure 4(B), it was possible to calculate the absorption coefficient $k\ (cm^{-1}) = (1/0.9)\ln(I_0/I_9)$ for any wavelength in the spectral interval under consideration. The result of this calculation appears to reproduce the experimental absorption spectrum satisfactorily, as shown in figure 4(A). However, the origin of the reabsorbing centres is far from clear. Ce^{3+} ions at regular sites cannot be involved in this process, since a self-absorption process would not result in a loss of the overall $5d \rightarrow 4f$ fluorescence. The fast and very weak broad fluorescence peaking around 420 nm observed under laser excitation at 355 nm (figure 2) most probably originates from Ce^{3+} ions at perturbed sites. These centres may well reabsorb the fluorescence emitted by Ce^{3+} ions at regular sites and act as quenching centres. On the other hand, the centres responsible for the red emission at 600 nm can hardly be involved in the reabsorption process, since they are not efficiently excited in the 320–380 nm spectral interval. However, they can act as electron–hole traps which may kill the scintillation process, since the excitation spectrum of the red emission originating from these centres exhibits an excitonic peak at 150 nm.

3. Light yield measurements

3.1. Cerium concentration dependence and time effects

For light yield measurements under γ-ray excitation, the samples were mounted onto the window of a Philips XP2020Q photomultiplier tube (PMT) using a liquid coupling grease and wrapped with Teflon. A ^{57}Co source emitting 122 keV γ-rays was used for irradiation. We also used ^{241}Am and ^{137}Cs sources. The light yields in photons per MeV did not significantly differ from the values obtained with the ^{57}Co source. As usually, the light yield was measured from the position of the photopeak using the single-electron spectrum for calibration. Measurements were also performed using a Hamamatsu S5345 avalanche photodiode.

The dependence of the light yield on the Ce concentration for the large samples 1–3 is displayed in figure 5. Different shaping times, ranging from 200 ns to 10 μs, were used. The light yields are observed to reach a saturation level when the dopant level exceeds 0.5%. Also, increasing the shaping time results in an increase of the light yield, which means that a slow component contributes significantly to the fluorescence decay under high-energy excitation.

Light yield measurements were performed under continuous x-ray excitation as well. Under these conditions of excitation, the light yield is obtained by comparison with that

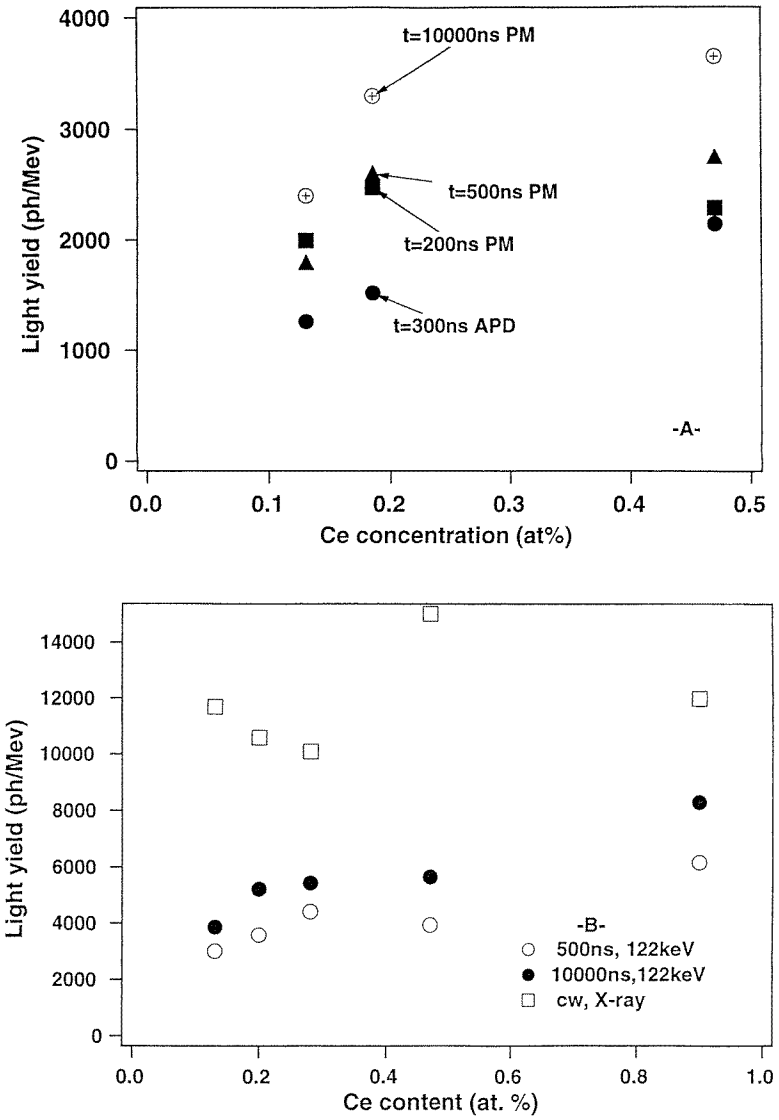

Figure 5. (A) Light yields of large samples (1–3) measured in the up position with different shaping times (no corrections have been applied for absorption of the luminescence). (B) Light yields of thin samples under x-ray and γ-ray excitation (x-ray data are corrected for absorption of the luminescence, but γ-ray data are not).

of a BaF_2 sample, which is 11 000 photons MeV^{-1}. For each sample, the x-ray-induced emission spectrum was divided by the transmission spectrum to account for reabsorption processes. In fact, the transmission spectrum was measured using a parallel beam while the x-ray induced fluorescence may enter the monochromator after multiple reflections on the crystal faces. Due to the large size of some of our samples, the corrected light yields are affected by an uncertainty which may be as large as 50%. These light yields are reported in table 2. Measurements were also performed on thin samples for which reabsorption is not significant.

Table 2. Light yields (photons MeV^{-1}) of different $LuAlO_3:Ce^{3+}$ samples with different shaping times (the specifications of these samples are given in table 1).

Sample No	122 keV 200 ns	122 keV 500 ns	122 keV 10 μs	122 keV[a] 300 ns	X-ray excitation cw
1	1996	1800	2400	1263	12 000
2	2472	2600	3300	1522	9 000
3	2288	2750	3650	2142	11 500
6		3018	3867		11 700
7		3595	5214		10 600
8		4413	5441		10 100
9		3954	5651		15 000
10		6170	8300		12 000

[a] The data in this column correspond to measurements using an avalanche photodiode.

The data in table 2 clearly show that light yields measured under cw x-ray excitation are always larger than those measured under γ-ray excitation. An explanation may be found in the presence of a long-decay-time luminescence component. This signal contribution is not observed if shaping times shorter than 10 μs are used in the measurements. Also the difference between γ-ray and x-ray intensity may play a role. The x-ray source delivers a much higher photon flux. Per second, we have approximately 10^9 x-ray quanta of, on average, 20 keV on a sample area of about 12 mm^2. At higher intensities, we may be confronted with filling of traps, thus reducing the loss probability. To check on this, we carried out some measurements on the time dependence of the light yield at high x-ray fluxes, using a 0.28% Ce-doped sample analogous to sample 8.

Upon switching on the x-ray irradiation, we observed that the scintillation intensity continues to increase well beyond the time at which the x-ray source has reached its maximum intensity. The light yield was increased by 50% within about 15 ms after this time. Furthermore, scintillation light was still emitted after the x-ray intensity had dropped to zero, with a decay time of about 10 ms, i.e. about the same as the rise time of the above 50% increase. In addition, there was a weak component of the order of 1 s. The process was reproduced each time we switched the x-ray tube on and off. Moreover, we observed an additional increase of 10% in about 200 s when we irradiated the sample for the first time after annealing at 400 °C for about 100 s. The decay of this increased yield has not yet been studied. We also observed the light yield as a function of the x-ray generator current. From first measurements, the light yield response appears to be non-linear, with an increase relative to the extrapolated linear response of the same order as the above 50% at the operation current of 25 mA.

From these results, the conclusion seems justified that traps play a role. With high-intensity x-ray irradiation, the traps are in equilibrium of filling and emptying, both with a $\cong$10 ms time constant. With many traps filled there is a more efficient direct transfer to the Ce luminescence centres and consequently an increased light yield. Under γ-ray excitation electrons and holes are also trapped, but at low radiation intensity the fraction of these trapped electrons and holes per absorbed γ-ray quantum will be higher and consequently the light yield will be lower. Yet, these trapped electrons and/or holes may result in luminescence once released from the shallow traps, thus giving rise to an afterglow. If the traps are involved in a quenching mechanism, this afterglow will have a reduced intensity. There is also an indication in the decay curves (recorded under γ-ray excitation) for long-time components. The possible role of the above 1 s and 200 s phenomena in a slow response is not clear yet.

Assuming that the traps are involved in quenching, the trap model may also explain that light yields measured under γ-ray excitation depend on the cerium doping level, while those measured under cw x-ray excitation do not. As discussed above, the magnitudes of photon fluxes from x-ray and γ-ray sources strongly differ. Since the samples were grown under the same experimental conditions, one may assume that the concentration of trapping centres does not vary significantly from one sample to the other. Under x-ray excitation, the photon flux is sufficiently high to ensure the filling of all the traps. If the traps are involved in quenching, the light yield no longer depends on the competition between energy transfers from electron–hole pairs either to Ce^{3+} ions or quenching centres. In opposition to this situation, the two energy transfer channels compete at very low photon fluxes and the light yield depends on the probability for a Ce^{3+} ion to be able to participate in the energy transfer.

3.2. Size effects

As previously discussed, in large crystals, a significant fraction of the scintillation light is absorbed in the sample itself. This may explain part of the difference in the data for the light yields of $LuAlO_3$:Ce^{3+} materials previously reported. In order to analyse the effect of the sample size on the light yield, we performed a series of measurements on sample 4 ($5 \times 5 \times 16$ mm^3), reducing each time its length by removing a thin slice. The sample was mounted with one of its small faces (face A) or one of its large faces (face B) onto the PMT window. In what follows, these two positions are referred to as up and down positions, respectively. For each series of measurements, the same face, either A or B, was against the PMT window. As previously reported, the light yield measured in the down position is always higher than in the up position [12]. One may argue that this effect is due to different coupling conditions. At the end of the series of measurements, as many thin slices were available, three of them, coming from different parts of the initial crystal, were selected and polished. We used the first and last slice and one from the middle part of the sample. The light yields of these three slices were measured and found to be almost identical. This shows that our result is hardly affected by parasitic effects such as fluctuations of the cerium concentration, differences in the quality of the optical contact, polishing or wrapping. The light yields were measured using 662 keV γ-rays from a ^{137}Cs source. The shaping time was 2 μs and a BGO sample was used as the reference. The result of these experiments is summarized in figure 6. The effect of the reabsorption process is dramatic since the light yield decreases from 110%–120% to 40% of BGO, when increasing the sample length from 0.5 to 16 mm. This problem is of great importance for applications to medical imaging devices, which require crystals with length not less than 40 mm. Moreover, such a reabsorption of the scintillation light will degrade the energy resolution. The light yield measured with the sample in the down position remains remarkably unaffected by the reduction of the sample length. The crossing point of the two curves displayed in figure 6 corresponds to a length of about 4.7 mm in the up position. This value appears to be very close to the corresponding length for the sample in the down position (5 mm). This is a test for the consistency of our data. This also means that the predominant parameter governing the reabsorption process is the length of the crystal. This is in agreement with the results shown in figure 4(B). The optical path followed by the fluorescent emission in the crystal depends on the position of the Ce^{3+} emitting centre in the crystal. Since the light yield measured for the sample in the down position does not depend significantly on its size, losses due to reflection on the lateral faces of the crystal may be assumed to be negligible.

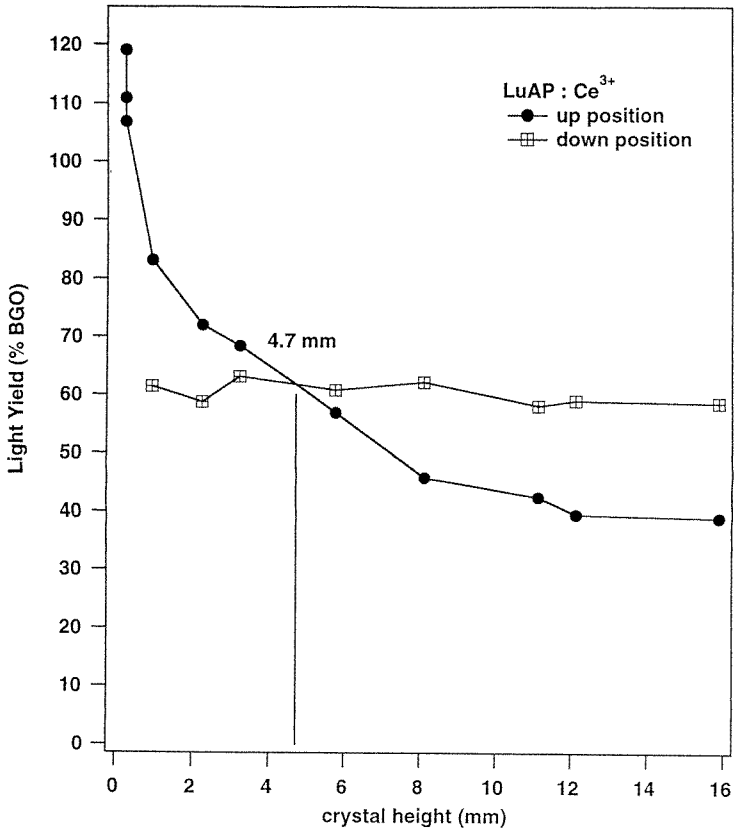

Figure 6. Effect of the size on the light yield. The light yield of a BGO sample is used as the reference. The length of sample 4 was progressively reduced by removing thin slices.

Very recently, a new large ($5 \times 5 \times 10$ mm^3) $LuAlO_3$ crystal, with an estimated cerium concentration of about 0.2 at.%, was cut from a boule grown in a pure molybdenum crucible. The light yield under γ-ray excitation measured for the sample in the up position was found to be about 4084 photons MeV^{-1}, i.e. 1.65 times that measured with the same shaping time for sample 2 (2472 photons MeV^{-1}) which has comparable specifications. This result shows that improving the light yield requires that efforts should be mainly focused on the crystal growth conditions.

4. Decay time measurements

Decay times of the scintillation under γ-ray excitation were measured using the start–stop method [17]. A ^{137}Cs source was used as the excitation source, and start and stop signals were detected using XP2020Q PMTs from Philips. The samples were mounted directly onto the window of the PMT generating the start signal and wrapped with Teflon in such a way as to allow fluorescence photons to reach the stop PMT through a small hole. If necessary, interference filters could be placed between the sample and the stop PMT. All the decays were observed to exhibit a fast component with a decay time of about 18.5 ns and a slow one in the range of 100 ns. Furthermore, a long non-exponential tail in the μs–ms range was

observed. The fast component originates from the fluorescence emitted by Ce^{3+} centres. The importance of the slow component can be characterized by the ratio R of the area of the decay distribution between 0 and 100 ns, and the area over the whole time interval (0-3 μs). The values of this ratio, measured for the thin samples, are reported in table 3. They are found to be of the order of 73% and do not depend significantly on the cerium doping level. Interference filters centred at either 350 or 370 nm were used to select the Ce^{3+} induced fluorescence in the case of sample 10, but no significant changes were observed. This shows that the slow component is really due to Ce^{3+} 5d $\rightarrow$ 4f radiative transitions and not to some other emitting centres or other transitions. The observation of a long non-exponential tail may explain part of the discrepancies observed between light yields measured under γ- and cw x-ray excitations. As previously reported, a slow component appears as soon as electron–hole pairs are created, while excitonic energy transfers to Ce^{3+} ions do not induce such slow components [16]. The data displayed in table 3 show that in the 0-3 μs time interval the competition between energy transfers from electron–hole pairs, on one hand, and excitons, on the other hand, does not depend on the cerium concentration in the 0.13–0.90 at.% range. Most probably, this range is not large enough to allow significant variations to be observed.

Table 3. Ratios R of the area under the decay pattern between 0 and 100 ns and the area over the whole time interval (0–3 μs) for $LuAlO_3$:Ce^{3+} thin samples under γ-ray excitation (the specifications of the samples are given in table 1).

	6	7	8	9	10
R (%)	72 ± 4	71 ± 6	73 ± 10	70 ± 6	75 ± 2

5. Main conclusions

The light yield of $LuAlO_3$:Ce^{3+} single crystals is shown to be predominantly governed by the size of the sample, due to a reabsorption process. A detailed analysis of size effects clearly shows that increasing the sample length from 0.5 to 10 mm results in a loss of about 70% of the scintillation efficiency. The origin of this process, however, is not clear, since the nature of the centres responsible for the absorption of the Ce^{3+} fluorescence could not be ascertained.

The discrepancies observed between the light yields measured under γ- and cw x-ray excitations are explained partly by the contribution of a slow component to the fluorescence decay. Also saturation of trapping centres when the photon flux is sufficiently high may also favour the fluorescence induced by cw x-ray excitation, which does not appear to depend on the cerium doping level. Light yields under γ-ray excitation are assumed to be controlled by the competition between energy transfer processes from electron–hole pairs to either Ce^{3+} ions or quenching centres.

Due to the low distribution coefficient of cerium in this system, it is hard to increase the cerium concentration over 1 at.%. Since the cerium concentration has no dramatic effect on the light yield in the range 0.1–1 at.%, efforts in improving the scintillation properties of the material under investigation should mainly focus on the crystal growth conditions. The light yield was shown to be increased by a factor of two by simply using a new Mo crucible.

Acknowledgments

Partial support by the EU commission under contract No CHRX-CT 93-0108, by NATO under contract No HTECH. CRG 940932 and by the Netherlands Technology Foundation (STN) is gratefully acknowledged.

References

[1] Baryshevsky V G, Kondratiev D M, Korzhik M V, Kachanov V A, Minkov B I, Pavlenko V B and Fyodorov A A 1993 *Nucl. Tracks. Radiat. Meas.* **22** 11
[2] Minkov B I 1994 *Functional Mater.* **1** 103
[3] Moses W W, Derenzo S E, Fyodorov A, Korzhik M, Gektin A, Minkov B and Aslanov V 1994 *IEEE Trans. Nucl. Sci.* **NS-42** 275
[4] Lempicki A, Randles M H, Wisniewski D, Balcerzyk M, Brecher C and Wojtowicz A J 1994 *IEEE Trans. Nucl. Sci.* **NS-42** 280
[5] Dujardin C, Pedrini C, Bouttet D, Verweij J W M, Petrosyan A G, Belsky A, Vasil'ev A, Zinin E I and Martin P 1996 *Proc. Int. Conf. on Inorganic Scintillators and their Applications (SCINT95) (Delft, 28 August–1 September 1995)* (Delft: Delft University Press) p 336
[6] Lempicki A, Brecher C, Wisniewski D and Zych E 1996 *Proc. Int. Conf. on Inorganic Scintillators and Their Applications (SCINT95) (Delft, 28 August–1 September 1995)* (Delft: Delft University Press) p 340
[7] Mares J A, Nikl M, Chval J, Kvapil J, Giba J and Blazek K 1996 *Proc. Int. Conf. on Inorganic Scintillators and Their Applications (SCINT95) (Delft, 28 August–1 September 1995)* (Delft: Delft University Press) p 344
[8] Moszynski M, Volski D, Ludziejenski T, Lempicki A, Brecher C, Wisniewski D and Wojtowicz A J 1996 *Proc. Int. Conf. on Inorganic Scintillators and Their Applications (SCINT95) (Delft, 28 August–1 September 1995)* (Delft: Delft University Press) p 348
[9] Trower W P, Korzhik M V, Fyodorov A A, Smirnova S A and Aslanov V A 1996 *Proc. Int. Conf. on Inorganic Scintillators and Their Applications (SCINT95) (Delft, 28 August–1 September 1995)* (Delft: Delft University Press) p 355
[10] Petrosyan A G and Pedrini C 1996 *Proc. Int. Conf. on Inorganic Scintillators and Their Applications (SCINT95) (Delft, 28 August–1 September 1995)* (Delft: Delft University Press) p 498
[11] Mares J A, Nikl M, Chval J, Dafinei I, Lecoq P and Kvapil J 1995 *Chem. Phys. Lett.* **241** 311
[12] Dujardin C, Pedrini C, Meunier-Beillard P, Moine B, Gâcon J C and Petrosyan A 1997 *J. Lumin.* **72–74** 759
[13] Dujardin C, Pedrini C, Gâcon J C, Petrosyan A G, Belsky A N and Vasil'ev A N 1997 *J. Phys.: Condens. Matter* **8** 5229
[14] Pedrini C, Belsky A N, Vasl'ev A N, Bouttet D, Dujardin C, Moine B, Martin P and Weber M J 1994 *Mater. Res. Soc. Symp. Proc.* vol 348 (Pittsburgh, PA: Materials Research Society) p 225
[15] Gumanskaya E G, Egorcheva O A, Korzhik M V, Smirnova S S, Povlenko V B and Fedorov A A 1992 *Opt. Spectrosc.* **72** 215
[16] Baryshevsky V G, Korzhik M V, Minkov B I, Smirnova S A, Fyodorov A A, Dorenbos P and van Eijk C W E 1993 *J. Phys.: Condens. Matter* **5** 7893
[17] Moses W W 1993 *Nucl. Instrum. Methods* **336** 253